

## Supporting Information

### **An extremely safe and wearable solid-state zinc ion battery based on a hierarchical structured polymer electrolyte**

Hongfei Li<sup>1†</sup>, Cuiping Han<sup>2†</sup>, Yan Huang<sup>1</sup>, Yang Huang<sup>3</sup>, Minshen Zhu<sup>1</sup>, Zengxia Pei<sup>1</sup>, Qi Xue<sup>1</sup>,  
Zifeng Wang<sup>1</sup>, Zhuoxin Liu<sup>1</sup>, Zijie Tang<sup>1</sup>, Yukun Wang<sup>1</sup>, Feiyu Kang<sup>2</sup>, Baohua Li<sup>2</sup>, Chunyi Zhi\*<sup>1,4</sup>

<sup>1</sup>Department of Materials Science and Engineering, City University of Hong Kong, 83 Tat Chee Avenue, Kowloon, Hong Kong 999077, China.

<sup>2</sup>Engineering Laboratory for Next Generation Power and Energy Storage Batteries, Engineering Laboratory for Functionalized Carbon Materials, Graduate School at Shenzhen, Tsinghua University, Shenzhen 518055, China

<sup>3</sup>College of Materials Science and Engineering, Shenzhen University, Shenzhen 518000, China.

<sup>4</sup>Shenzhen Research Institute, City University of Hong Kong, Nanshan District, Shenzhen 518057, China.

<sup>†</sup>The authors contribute equally to this work.

\*e-mail: cy.zhi@cityu.edu.hk

## **Materials and Methods**

### **Preparation of PAN fiber membrane**

PAN fiber membrane was fabricated through a facile electrospinning method by using an electrospinning machine (SS-2535, Beijing Ucalery Co., Ltd.). 15 wt% PAN ( $M_w = 150\,000$ , J&K Scientific Ltd.) was dissolved in N,N -dimethylformamide (DMF) with continuous stirring at 70 °C for 6 h, followed by an ultrasonic treatment for 1 h. After that, the PAN solution was sequentially electrospun onto the rotating collector with a flow rate of 1.0 mL h<sup>-1</sup>. The obtained PAN fiber membrane was removed from the collector and dried at 60 °C for 4 h under vacuum for further use.

### **Preparation of HPE and GE**

HPE was synthesized by an in situ synthesis approach. In a typical experimental run, 2 g commercial gelatin (photographic grade, Aladdin) and 15 mg potassium persulfate were added to 20 mL mixture solution of 1 mol L<sup>-1</sup> ZnSO<sub>4</sub> (AR grade, Sigma) and 0.1 mol L<sup>-1</sup> MnSO<sub>4</sub> (AR grade, Sigma), followed by extensive stirring at 80 °C until all the gelatin and potassium persulfate was dissolved. 3 g acryl amide (AR grade, Aladdin) and 2 mg N,N'-methylenebisacrylamide (CP grade, Aladdin) were sequentially added to the above solution. After that, the mixture was stirred at 40 °C for 2 h, evacuated, and injected into an electrospun PAN membrane and heated at 60 °C for 2~3 h. Then, a crosslinked 3D framework structure filled by gelatin/PAM-based solid electrolyte was formed in the electrospun PAN membrane pores. Finally, the as-prepared polymer film was soaked in a mixed solution of 2 mol L<sup>-1</sup> ZnSO<sub>4</sub> and 0.1 mol L<sup>-1</sup> MnSO<sub>4</sub> for 1 h to achieve the equilibrated state. For comparison, GE film was prepared by adding 2g pristine gelatin to 15 mL mixture solution of 1 mol L<sup>-1</sup> ZnSO<sub>4</sub> and 0.1 mol L<sup>-1</sup> MnSO<sub>4</sub>, followed by extensive stirring at 80 °C until the gelatin was dissolved. Then GE film was obtained by a simple casting method.

### **Preparation of MnO<sub>2</sub> cathode**

MnO<sub>2</sub>/CNT composite was synthesized by a modified co-precipitation and hydrothermal method. In a typical synthesis run, 0.15 g commercial multi-walled CNT with a diameter of 10~30 nm and a length of 5~10 μm (Shenzhen Nanotech Port Co., Ltd.) was purified by refluxing the as-received sample in nitric acid (AR grade, 68 wt%, Aladdin) for 6 h at 80 °C. The acid-treated CNT was washed with deionized water several times and finally re-dispersed in 150 mL deionized water. Then, 2.94 g Mn(CH<sub>3</sub>COO)<sub>2</sub> · 4H<sub>2</sub>O (AR

grade, Aladdin) was added into the above solution under continuous stirring for 0.5 h. Subsequently, the above solution was added drop-wise into an aqueous solution prepared by dissolving 1.27 g  $\text{KMnO}_4$  (AR grade, Aladdin) into 80 mL deionized water and stirring for 0.5 h. The mixed solution was then blended intensively by an ultrasonic mixer for 10 min and transferred to a Teflon-lined autoclave and heated at 120 °C for 12 h. After cooling, the obtained dark brown precipitate was washed several times by deionized water and dried at room temperature in a vacuum oven for 8 h to finally obtain the  $\text{MnO}_2/\text{CNT}$  composite.

To prepare the cathode,  $\text{MnO}_2/\text{CNT}$  composite, acetylene blacks and polytetrafluoroethylene (PTFE) binder were mixed in a weight ratio of 7:2:1 with deionized water as solvent. The mixtures were then stirred for 3 h and coated on a piece of CNT paper (Suzhou TanFeng Technology Co., Ltd.). Finally, they were dried at 40 °C in vacuum and cut into small electrodes (size 1 cm×1 cm). The effective mass loading of  $\text{MnO}_2$  is about 1.0-2.5 mg  $\text{cm}^{-2}$ .

### **Preparation of Zn anode**

Flexible Zn electrode was prepared by a facile electrochemical deposition method on the CNT paper substrate. A typical two-electrode setup was used for Zn electroplating, in which CNT paper substrate was used as working electrode, while zinc plate (purity > 99.99%, Sigma) was used as both counter and reference electrode. Aqueous solution containing 1 mol  $\text{L}^{-1}$   $\text{ZnSO}_4$  (AR grade, Sigma) and 1 mol  $\text{L}^{-1}$   $\text{KCl}$  (AR grade, Sigma) was used as electrolyte. Electroplating was performed at 10 mA  $\text{cm}^{-2}$  for 2000 s using an electrochemical workstation (CHI 760D). The effective mass loading of zinc is about 3.0-5.0 mg  $\text{cm}^{-2}$ .

### **Characterization methods**

Structural and phase characterizations of the as-prepared solid electrolytes film and electrodes were done by XRD using a Bruker D2 Phaser diffractometer with  $\text{Cu K}\alpha$  irradiation ( $\lambda = 1.54 \text{ \AA}$ ). The surface morphology of these samples was characterized by an environmental scanning electron microscope (ESEM, FEI/Philips XL30). The morphology and microstructure of the samples were revealed by a JEOL-2001F field-emission TEM.

### **Electrochemical measurements**

Cyclic voltammetry (CV) curves and electrochemical impedance spectroscopy (100 kHz to 0.1 Hz) were conducted by an electrochemical workstation (CHI 760D). The CV curves of ZIBs were measured based on two-electrode system, in which Zn was used as both counter and reference electrodes (negative

electrode) and MnO<sub>2</sub> cathode was used as work electrode (positive electrode). Electrochemical performance of the prepared ZIB was examined based on galvanostatic testing of CR2032-type coin cells (for aqueous ZIBs) and planar thin film battery (for solid-state ZIBs) in the voltage range of 0.85 V -1.9 V using a Land 2001A battery testing system at 24 °C. The area of solid-state ZIB is about 7 cm<sup>2</sup> and the thickness is around 0.11 mm.

The areal energy density (E) of the full battery was calculated by:  $E = \int_0^t IV_{(t)} dt / A$ ,  $P = E/t$ , where  $I$  is the discharge current,  $V(t)$  is the discharge voltage at  $t$ ,  $dt$  is time differential and  $A$  is the total areal of the whole solid-state device (including anode, cathode and polymer electrolyte, etc.). Here,  $I = 2772 \text{ mA} = 2.772 \text{ A}$ ,  $t = 150 \text{ s} = 0.0417 \text{ h}$ ,  $A = 7 \text{ cm}^2$ ,  $E = \int_0^t IV_{(t)} dt / A = \int_0^{0.0417} 2.772 V dt / 7 = 0.00618 \text{ Wh/cm}^2 = 6.18 \text{ mWh/cm}^2$ , and  $P = E/t = 0.00618 / 0.0417 \text{ W/cm}^2 = 148.2 \text{ mW/cm}^2$ .

### **Wearable Demonstration**

A commercial smart watch with Android system was used to do the smart watch demonstration. Before the operations, the original watch battery has been removed. Then, three solid-state ZIBs (size 4.0 cm×6.0 cm×0.1cm) based on HPE were charged to 1.8V and connected in series. Finally, they were attached to the smart watch to for the demonstration.

The health monitoring was constructed by a pulse sensor (Xinyuan Electronic Technology Co., Ltd.), an Arduino single-chip microcomputer (Xinyuan Electronic Technology Co., Ltd.) and ZIBs. Four solid-state ZIBs (size 2.0 cm×6.0 cm×0.1cm) were charged to 1.8V and connected in series, after which they were laid in a T-shirt to power the pulse sensor under both flat and bending conditions. The pulse signal waveform was collected by the pulse sensor and processed by Arduino single-chip microcomputer and then sent to computer for data collection.

The plantar measurement system was constructed using a commercial smart insole and two solid-state ZIBs (size 2.7 cm×3.6 cm×0.1cm) placed under the insole. Two ZIBs were charged to 1.8V and connected in

series, followed by attaching with sensors of the smart insole. Then the smart insole together with these ZIBs were put into sports shoes and start the running and walking test. All the sport analysis results including gait, knee stress, contact flight ratio, and compressive evaluation were tracked by the insole and sent to a mobile phone through the Bluetooth module in the insole.

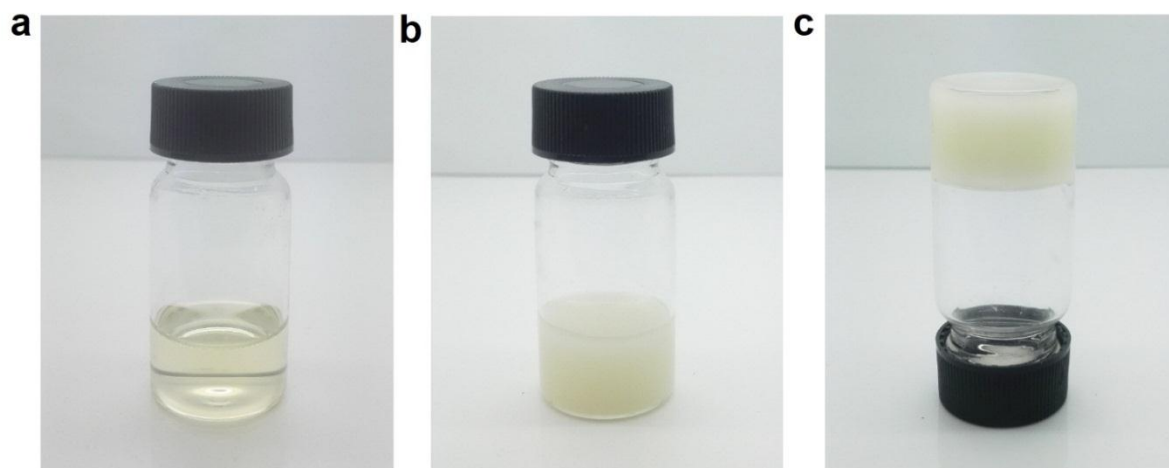


**Fig. S1 Optical images of aqueous and hydrogel electrolytes.** (a) Gelatin dissolved in the mixture solution of  $1 \text{ mol L}^{-1} \text{ ZnSO}_4$  and  $0.1 \text{ mol L}^{-1} \text{ MnSO}_4$ . (b), (c) Gelatin-g-PAM hydrogel prepared by the free radical polymerization approach.

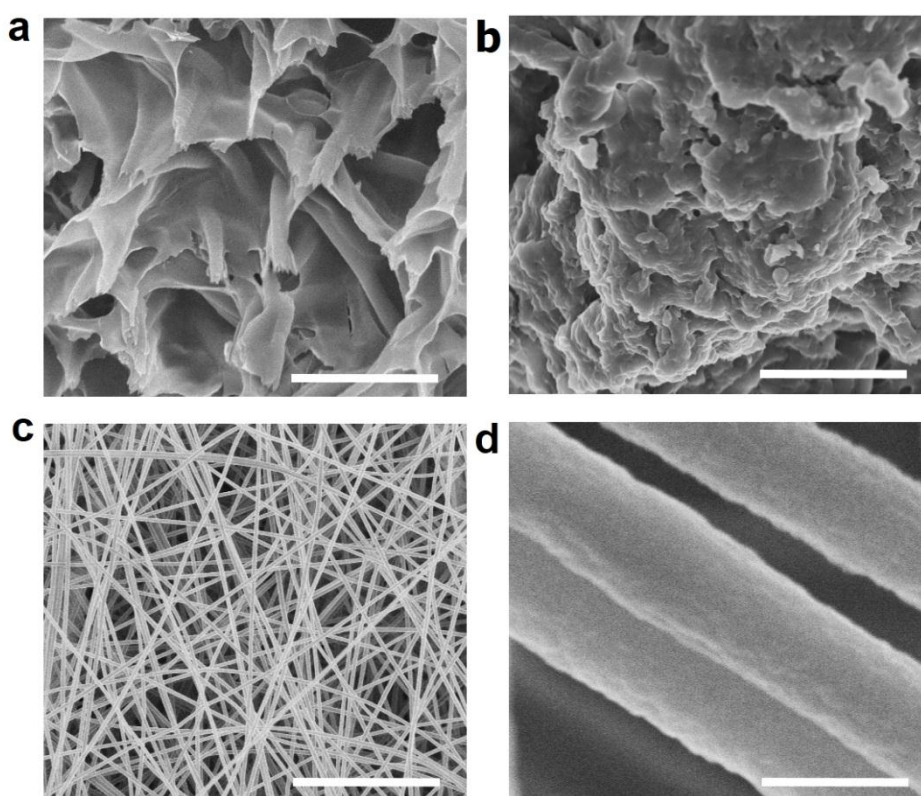


**Fig. S2 Morphology of HPE, GE and PAN fiber membrane.** (a) SEM image of HPE film. (b) SEM image of GE (pristine gelatin based electrolyte). (c), (d) SEM image of PAN electrospun fiber membrane. Scale bars,  $1 \text{ }\mu\text{m}$  (a),  $5 \text{ }\mu\text{m}$  (b),  $10 \text{ }\mu\text{m}$  (c) and  $500 \text{ nm}$  (d).

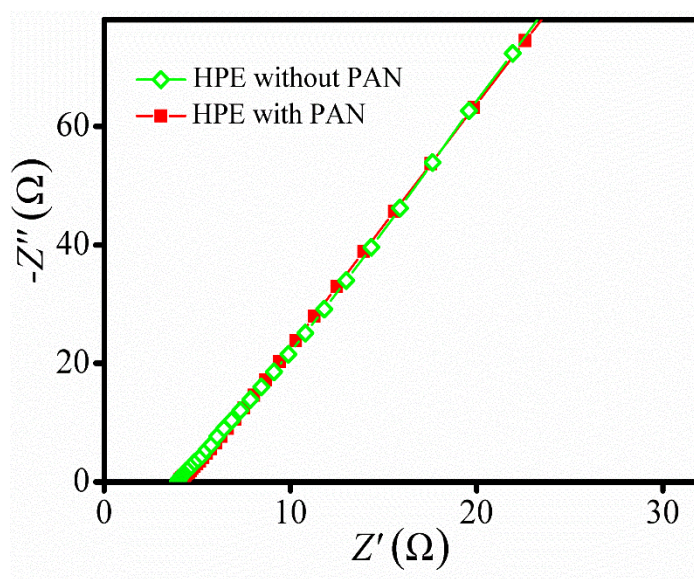


**Fig. S3 AC impedance spectra of the HPE without and with PAN membrane in the frequency range from 10 kHz to 0.01 Hz.**

We compared the ionic conductivity of HPE film without and with PAN. The ionic conductivity of HPE film without PAN showed an ionic conductivity of  $1.82 \times 10^{-2} \text{ S cm}^{-1}$  (Fig. 3), which is almost the same as the HPE film with PAN membrane. It indicates that The PAN membrane in HPE has no effect on the ionic conductivity of HPE film.

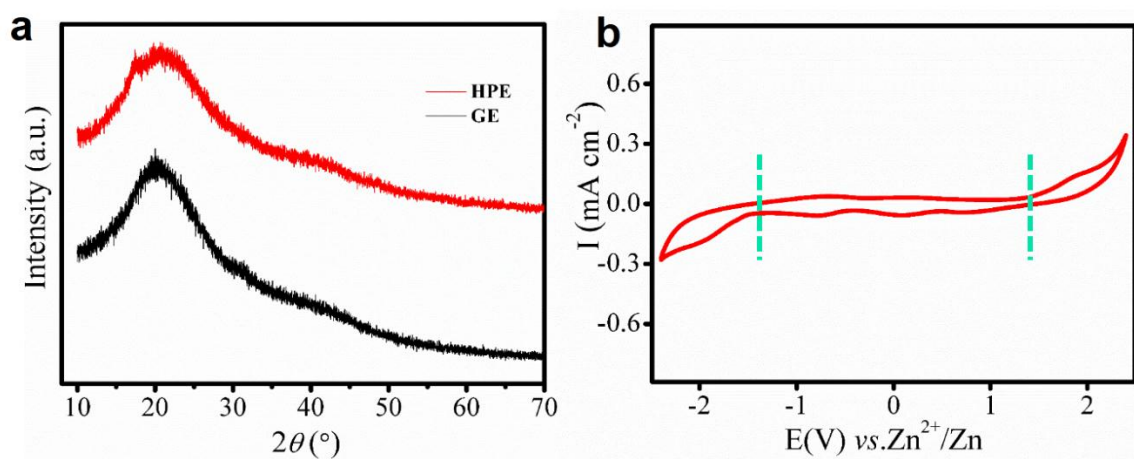


**Fig. S4 Characterization of HPE and GE.** (a) The X-ray diffraction patterns of the GE and HPE films. (b) Electrochemical stable window of HPE.

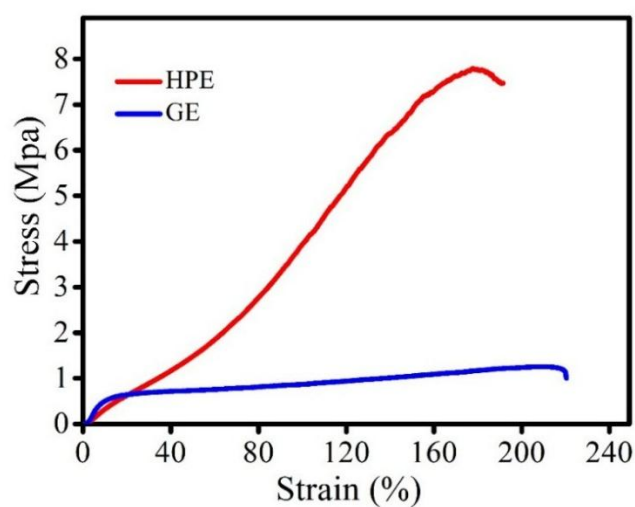


**Fig. S5 Stress–strain curves of the HPE and GE.** It is obvious that the HPE shows greatly enhanced tensile strength than GE.

**Table S1.** Comparison of HPE with some zinc-salt-polymer-electrolytes in terms of ionic conductivity in the literatures.

Polymer matrices	Ionic conductivity $\text{mS cm}^{-1}$	Zinc salts	Reference
HPE	17.6	$\text{ZnSO}_4$	<b>This work</b>
Gelatin	5.68	$\text{ZnSO}_4$	<b>This work</b>
PEO	0.5~0.8	$\text{ZnCl}_2$	<i>Solid State Ionics</i> , 2005, <b>176</b> , 1797.
PEO	2~4	$\text{ZnCl}_2$	<i>J. Electrochem.Soc.</i> , 2007, <b>154</b> , A554
Poly- $\epsilon$ -caprolactone	0.88	$\text{Zn}(\text{CF}_3\text{SO}_3)_2$	<i>Express Polym. Lett.</i> , 2013, <b>7</b> , 495
Poly(4-vinylpyridine)	$2 \times 10^{-5}$	$\text{Zn}(\text{ClO}_4)_2$	<i>Macromolecules</i> , 2004, <b>37</b> , 192
PAN	0.22	$\text{ZnSO}_4$	<i>J. New Mat. Electr. Sys.</i> , 2001, <b>4</b> , 135
PAN	0.78	$\text{ZnCl}_2$	<i>J. New Mat. Electr. Sys.</i> , 2001, <b>4</b> , 135

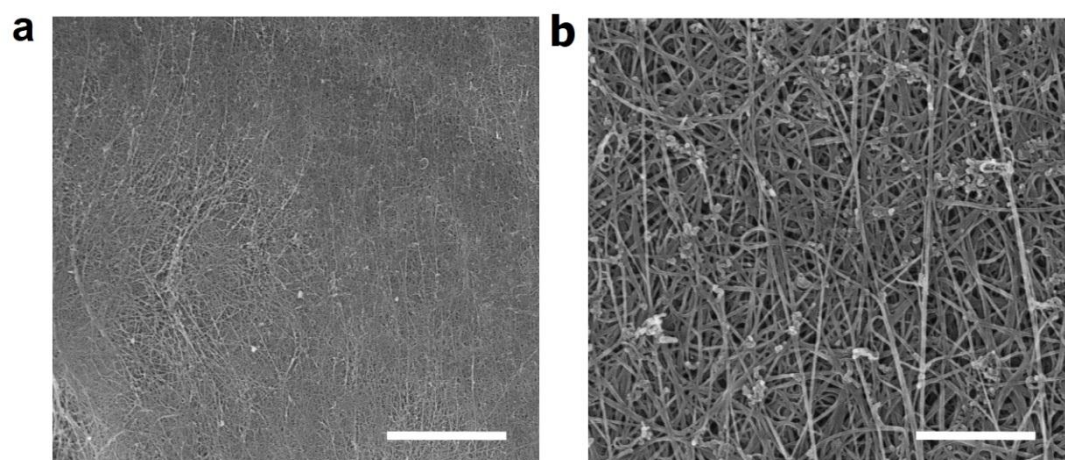


**Fig. S6 SEM images of CNT paper showing the non-woven structure of CNTs. Scale bars, 10  $\mu\text{m}$  (a), 1  $\mu\text{m}$  (b).**

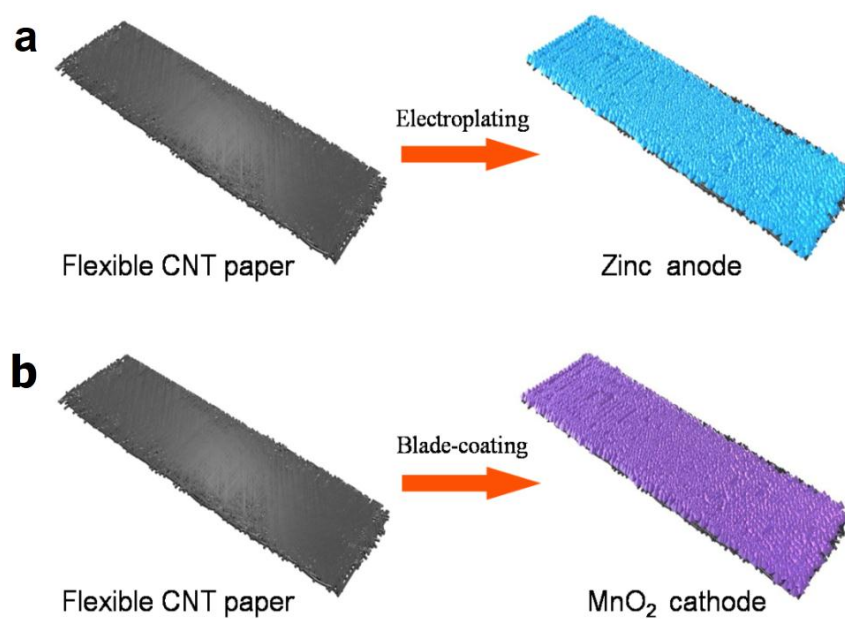


**Fig. S7 Schematic illustration of the preparation of flexible zinc anode (a) and  $\text{MnO}_2$  cathode (b).**

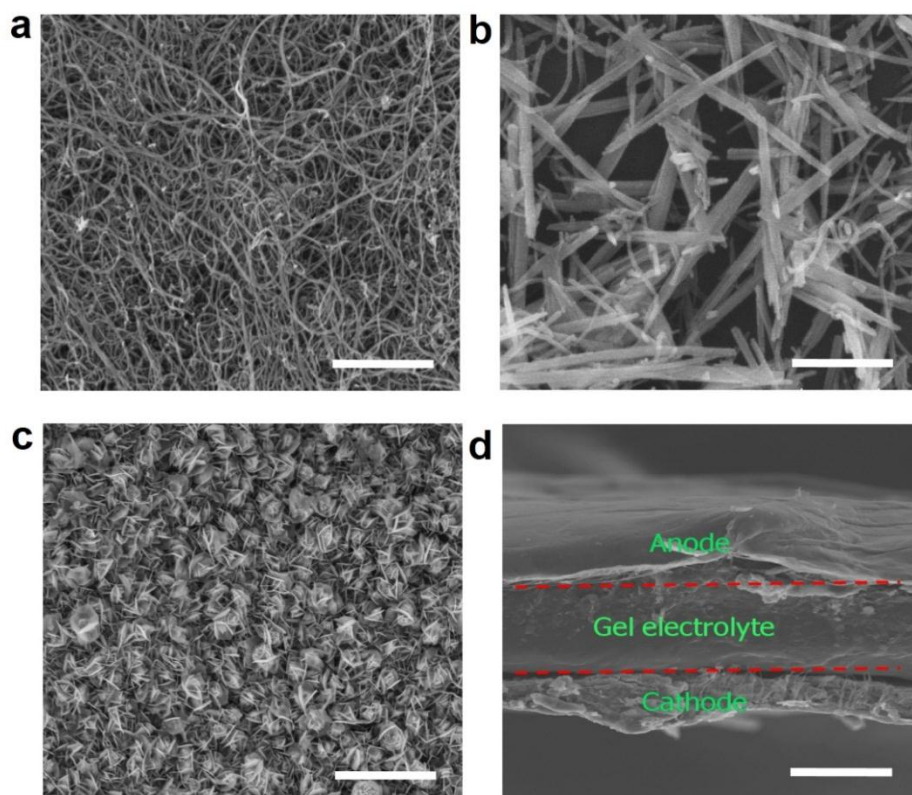


**Fig. S8 Morphology of CNT powder, zinc anode and ZIB.** (a) SEM image of acid-treated CNT used in the cathode. (b) SEM image of MnO<sub>2</sub> nanorods/CNT composite. (c) SEM image of electroplated zinc. (d) Cross-section SEM image of the as-prepared solid-state ZIB (without freeze-drying). Scale bars, 1  $\mu\text{m}$  (a), 200 nm (b), 8  $\mu\text{m}$  (c) and 80  $\mu\text{m}$  (d).

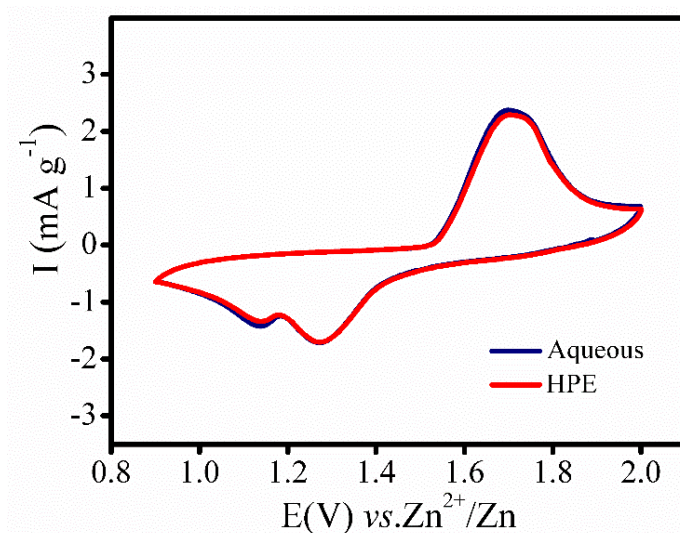


**Fig. S9** CV curves of ZIBs based on the aqueous electrolyte (1M ZnSO<sub>4</sub> and 0.1M MnSO<sub>4</sub>) and HPE polymer electrolyte at a scan rate of 1 mVs<sup>-1</sup>.

We have compared the CV curves of the ZIB based on the aqueous electrolyte (1M ZnSO<sub>4</sub> and 0.1M MnSO<sub>4</sub>) and our developed HPE polymer electrolyte at the same scan rate of 1 mVs<sup>-1</sup>. It can be seen that the ZIB with HPE polymer electrolyte showed similar CV curve compared with the ZIB with traditional aqueous electrolyte. The negligible variance in voltage difference between the anodic and cathodic peaks ( $E_p$ ) suggests the ZIB with HPE polymer electrolyte has similar voltage windows compared with the ZIB with traditional aqueous electrolyte.

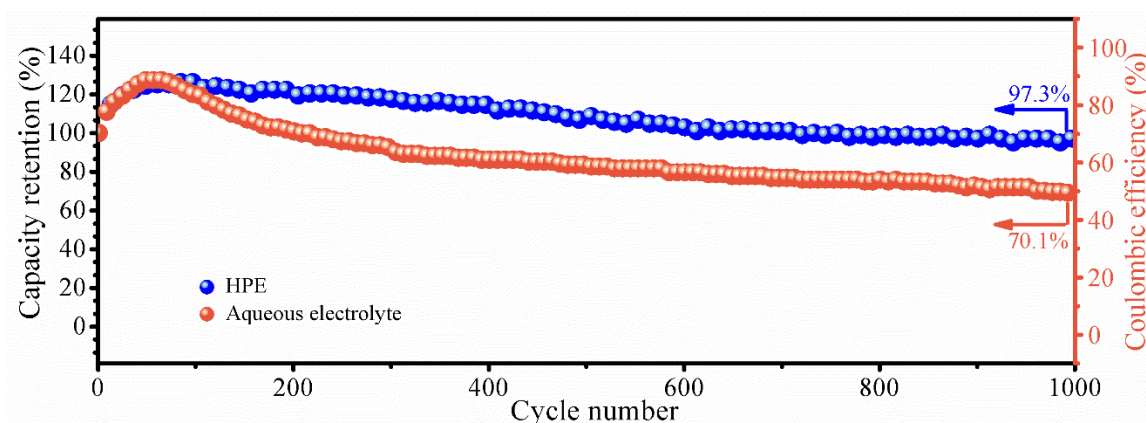


**Fig. S10** Comparison of cycling performance of ZIBs in aqueous mixed solution of 1M ZnSO<sub>4</sub> and 0.1M MnSO<sub>4</sub> and HPE polymer electrolyte at a same charge/discharge current of 2772 mA g<sup>-1</sup>.

The ZIB based on an aqueous solution showed a capacity retention of 70.1% after 1000 charge/discharge cycles, which is much poorer than the performance in solid-state HPE film (97.3%).

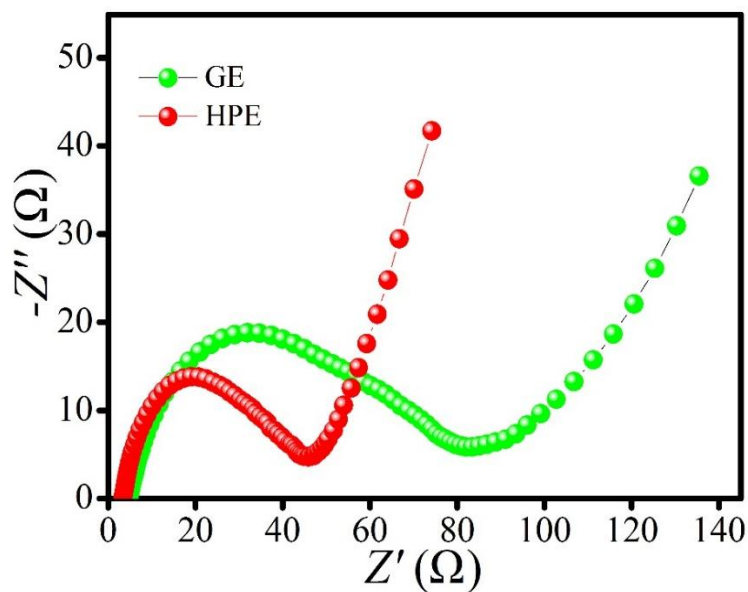


**Fig. S11 Electrochemical impedance spectroscopy (EIS) plots of solid-state ZIB based on the GE and HPE.** Impedances are measured at the second cycle in the frequency range from 10 kHz to 0.01 Hz (at the half charge state of 1.6 V).

Electrochemical impedance spectroscopy (EIS) results of ZIBs with gelatin and HPE were shown above. The intersection of the EIS plot with real axis at the high frequency reveals the bulk resistance ( $R_b$ ), while the medium-frequency semicircle represents the interfacial resistance between the solid electrolyte and electrodes ( $R_i$ ). It can be seen from the EIS plot that both  $R_b$  and  $R_i$  of the ZIB with HPE are lower than those of the ZIB based on pristine GE. This indicates that the hierarchical structured gelatin and PAM based polymer electrolyte is more effective to maintain a good electrode/electrolyte interface than the pristine gelatin electrolyte, which leads to a higher ion diffusion coefficient and faster electrochemical reaction kinetic.

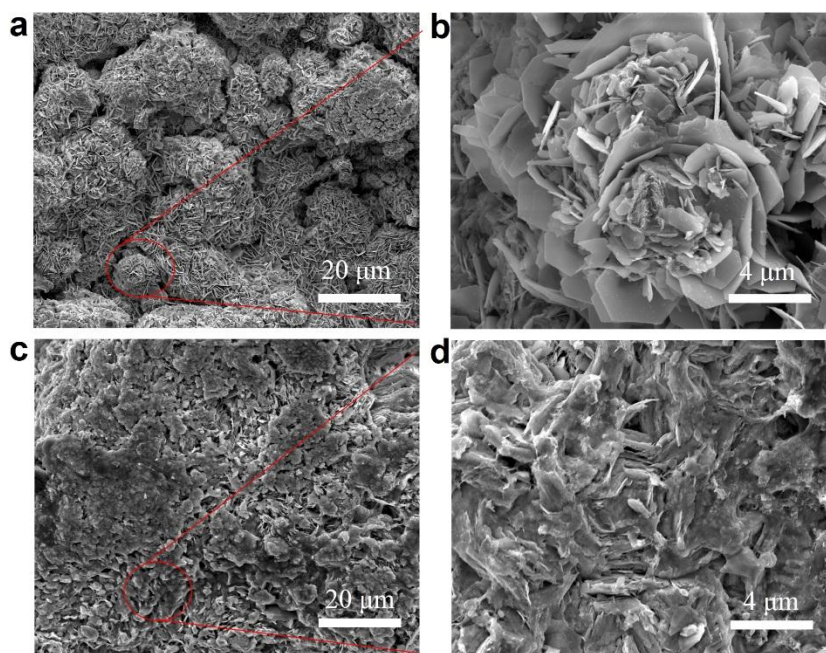


**Fig. S12** Morphology images of zinc anode after 500 cycles (at  $1848 \text{ mA g}^{-1}$ ) in aqueous electrolyte (a-b) and HPE (c-d).

It is true that Zn electrode favors to form dendrites during cycling. But due to different reaction mechanisms, the zinc dendrites formed in mild electrolyte is much less than that in alkaline solutions (*Nat. Energy* 2016, **1**, 16039). However, due to the uneven zinc plating/stripping process on the surface of zinc anode, the growth of Zn dendrites/protrusions is inevitable. To further suppress the formation of Zn dendrites/protrusions and enhance the reversibility of zinc anode, we use the developed gelatin/PAM/PAN based polymer electrolyte to replace the aqueous electrolyte. The highly reversible plating and stripping of zinc occurring in the interface between the polymer electrolyte and Zn anode is of great importance for the long-term cycling stability of rechargeable Zn/MnO<sub>2</sub> batteries.

The morphology images of zinc anode after 500 cycles in aqueous electrolyte and HPE were shown in Figure S13, respectively. For zinc electrode tested in aqueous electrolyte, zinc dendrite formation is observed on the surface of the post-cycled Zn anode, reflecting a very uneven Zn stripping/plating process. While for zinc electrode charged/discharged in our polymer electrolyte, the surface of the post-cycled Zn anode is much even and no obvious zinc dendrites were observed.

It is believed that dendrite growth is mainly induced by inhomogeneous distribution of zinc ions and current density on a current collector. With gelatin/PAM/PAN based polymer electrolyte, the electrostatic interaction between the positively charged Zn ions and negatively charged carboxylic acid groups along the

gelatin chains immobilized the Zn ions and facilitate the homogeneous distribution of Zn ions across the whole interface.

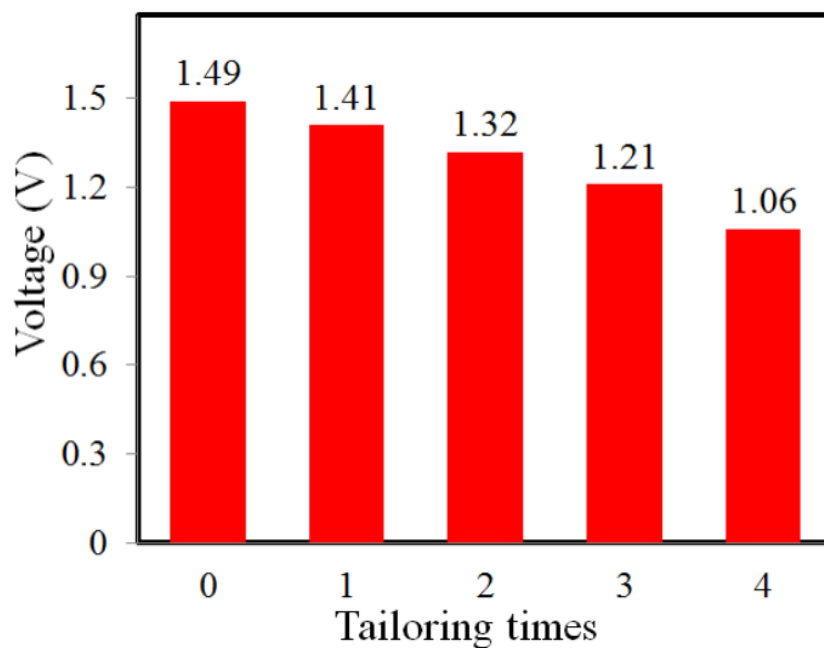


**Fig. S13 Cutting test of the ZIB based on aqueous electrolyte.** Here 1 mol L<sup>-1</sup> ZnSO<sub>4</sub> and 0.1 mol L<sup>-1</sup> MnSO<sub>4</sub> was used as the aqueous electrolyte for ZIB. Compared with the solid-state ZIB, the voltage of the ZIB based on traditional aqueous electrolyte decreased a lot after cutting.

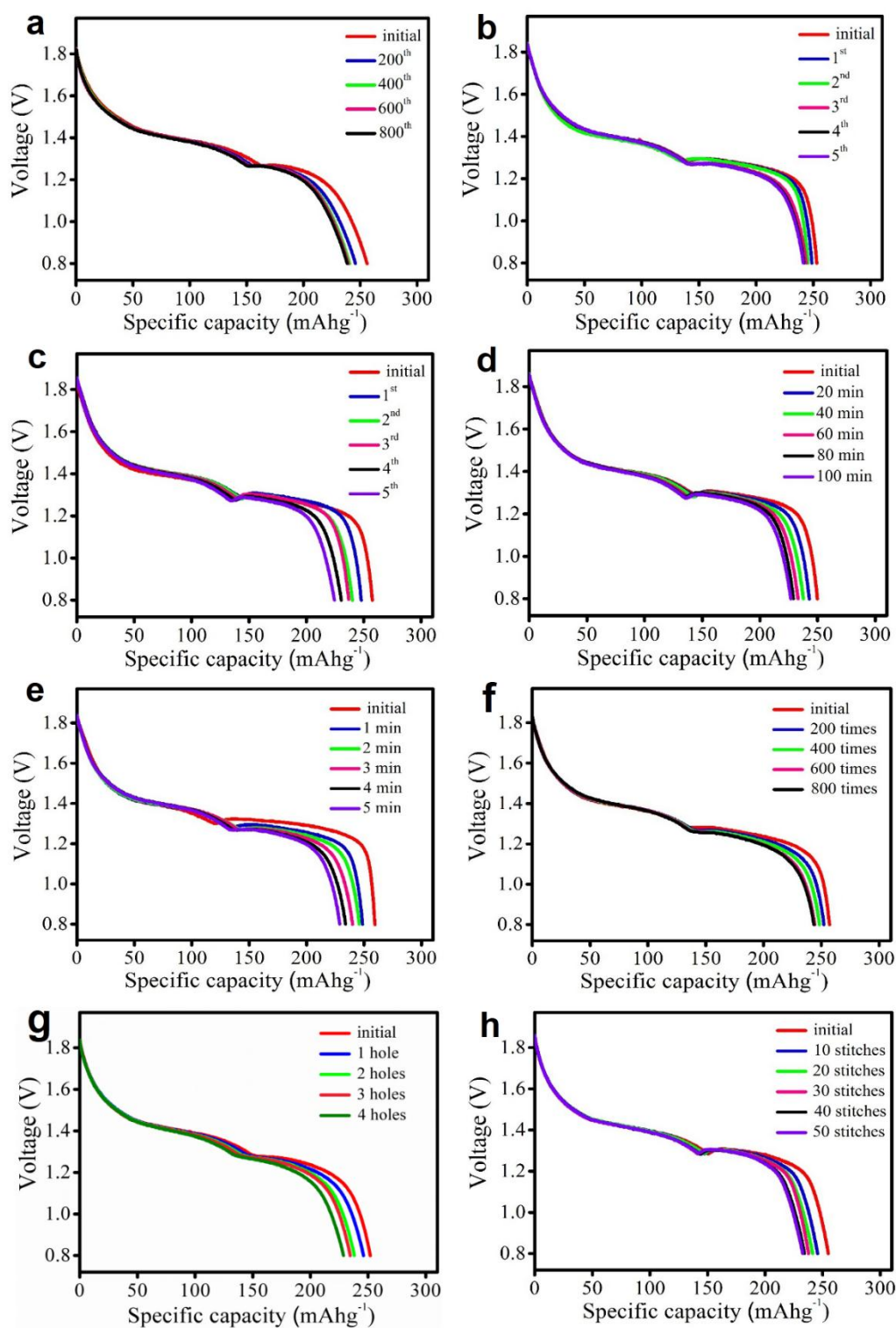


**Fig. S14 Discharge curves of the solid-state rechargeable ZIB under different destructive tests. (a)** Bending test. **(b)** Hammering test. **(c)** Combustion test. **(d)** Soaking test. **(e)** Washing test. **(f)** Weight loading test. **(g)** Drilling test. **(h)** Sewing test.

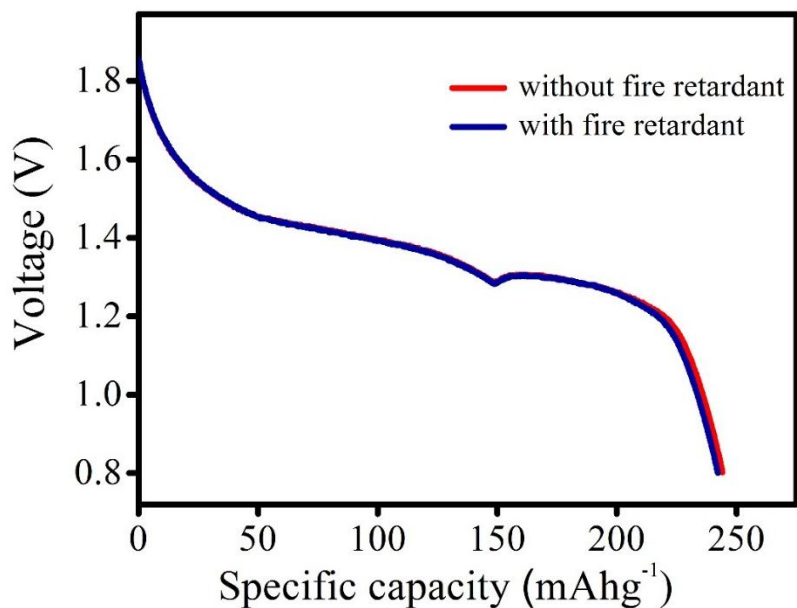


**Fig. S15 Discharge curves of the solid-state rechargeable ZIB before and after adding fire retardant in the electrolyte at 616 mA g<sup>-1</sup>.** Zinc borate (ZB) was added into the mixed solution of gelatin, ZnSO<sub>4</sub> and MnSO<sub>4</sub> before the polymerization of AM to prepare a ZB modified HPE (ZHPE), which followed a same synthesis route of HPE. After the unpackaged battery was assembled with ZHPE, a layer of ZB modified gelatin-g-PAM hydrogel was coated on the surface of ZIB. It can be seen that the ZIB showed very similar discharge capacity before and after adding fire retardant, indicating that the fire retardant does not noticeably affect the electrochemical performance of ZIB.

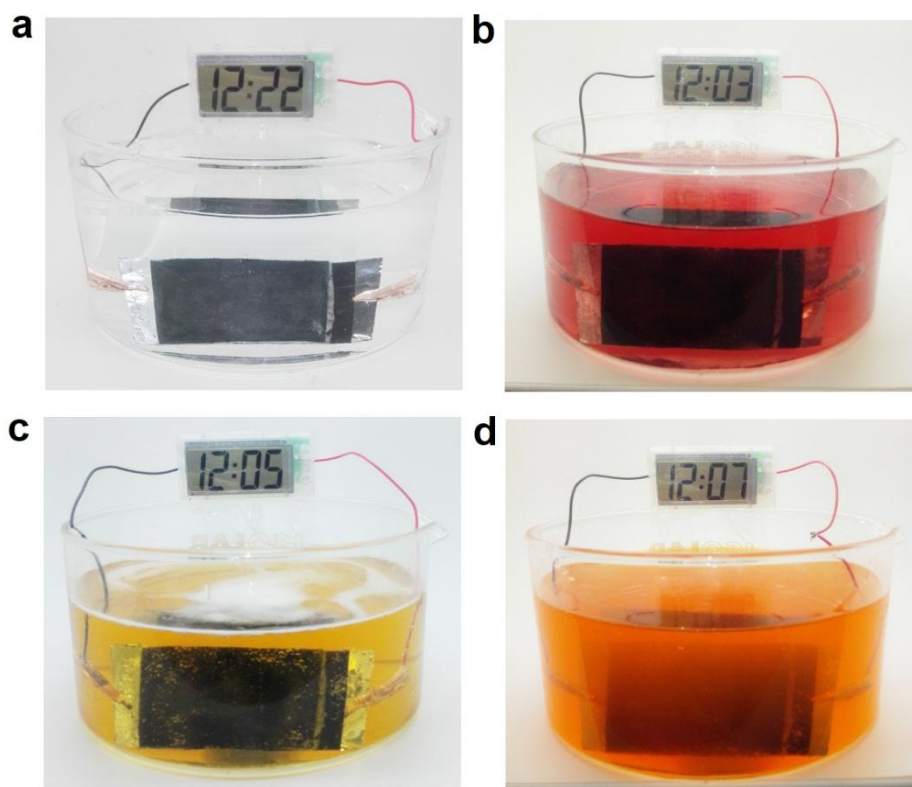


**Fig. S16 Soaking test of the solid-state rechargeable zinc ion battery in different solutions. (a)** DI water. **(b)** Redberry juice. **(c)** Beer. **(d)** Soda. The ZIB can operate well and power the electronic watch when soaking in different kinds of solutions.



**Fig. S17 Wearable applications of flexible solid-state ZIBs.** (a) Three ZIBs were connected in series to power a commercial smart watch. (b) Four ZIBs under bending condition were integrated in series to power a pulse sensor. (c) Step numbers (from the first day to the third day). These step numbers were got by the ZIB-powered smart insole in three days, during which we didn't charge the ZIBs and just used their initial power. (d) Compressive evaluation of the running results. (e) Strike type (the first one, from left to right), contact flight ratio (second), cadence result (third) and pronation result (fourth) obtained by the ZIB-powered smart insole.